Application of *ab initio* methods for calculations of voltage as a function of composition in electrochemical cells

J. N. Reimers and J. R. Dahn
Department of Physics, Simon Fraser University, Burnaby, British Columbia, Canada V5A 1S6
(Received 20 July 1992)

Results of *ab initio* total-energy calculations are used to calculate effective atom-atom interactions in a lattice-gas model for the binary alloy Li_xAl for $0 \le x \le 1$. The statistical mechanics is solved at finite temperature to obtain the *ab initio* chemical potential of lithium in Li-Al alloys as a function of composition x. We compare our calculated results with the experimentally measured chemical potential from an electrochemical cell. Predicting chemical potentials from first principles will be important for understanding technologically important intercalation compounds used for advanced battery applications.

I. INTRODUCTION

Ab initio total-energy calculations can be used to calculate the cohesive energy, the lattice constant and the bulk modulus of periodic solids.[1] The stability of one structural phase over another can be predicted, as can the phase diagrams of alloy systems.[2,3] Confidence in the theoretical predictions is attained when they are able to reproduce a wide body of experiments for a particular system. Although chemical potentials can be calculated using *ab initio* methods based on the cluster expansion method[4] just as phase diagrams can, to our knowledge there has not yet been a comparison between calculated and experimentally measured chemical potentials. The chemical potential of one or more components of alloy systems or the chemical potential of intercalated atoms in intercalation compounds is easily measured using electrochemical techniques, so such a comparison should be possible. Of course, comparisons have been made for phenomenological models based on lattice-gas models[5] with atom-atom interactions as adjustable parameters.

For an A-B alloy system, the voltage $V(y)$ of an electrochemical cell with pure A as one electrode and A_yB as the other electrode (and an electrolyte containing dissolved A^+ ions) is given by[6]

$$eV(y) = -[\mu'(y) - \mu_A], \tag{1}$$

where $\mu'(y)$ is the chemical potential of A in A_yB and μ_A is the chemical potential of A in pure A. To obtain this result, we assume the reactions at the electrodes are

$$\delta y\ A \rightarrow \delta y\ A^+ + \delta y\ e^-$$

at the A electrode and

$$A_yB + \delta y\ A^+ + \delta y\ e^- \rightarrow A_{y+\delta y}B$$

at the A_yB electrode. The voltage of Li/Li_yAl cells as a function of y has already been measured[7] and can be used to obtain the chemical potential of Li. Here we report our own measurements on Li/Li_yAl cells, which agree well with the earlier work.

To calculate the chemical potential $[\mu'(y)]$ of A in an A_yB alloy from first principles, one calculates total or cohesive energies for a number of "suitable" stable and metastable phases. From these energies, effective atom-atom interactions are derived in the context of an Ising-like or lattice gas model.[4] Then statistical mechanics is used to obtain an *ab initio* phase diagram, $\mu'(y)$ and μ_A. From the chemical potentials, the voltage of an A/A_yB electrochemical cell is obtained. Because the experiments measure cell voltage, not chemical potential, we will calculate the appropriate cell voltages.

Recently, intercalation compounds such as Li_yC_6 (Ref. 8) and Li_yNiO_2 (Ref. 9), Li_yCoO_2 (Ref. 10), or $Li_yMn_2O_4$ (Ref. 11) have been proposed and used in prototype high-energy-density rechargeable batteries. The search for even better batteries of this type is generally acknowledged to be a search for new materials with appropriate ranges for the chemical potential of lithium. In our laboratory, this search for new materials is made using chemical and physical intuition coupled with an active synthesis program. However, we often find that new materials, which we synthesize, give lithium chemical potentials that are not technologically interesting. An *ab initio* calculation done prior to synthesis, using methods similar to those that will be outlined below, could save hundreds of hours of experimental work and could point the way to interesting classes of materials. Now that the cost of computing is decreasing rapidly, while that of experiment is increasing, it is possible that calculations similar to those described below will be important in the selection of electrode materials for the next generation of advanced batteries.

At room temperature the experimental phase diagram[12] for Li_xAl_{1-x} indicates that the fcc aluminum structure is only stable for $0 \le x \le 0.01$, beyond which a phase coexistence between fcc Al and LiAl exists for $0.01 \le x \le \frac{1}{2}$. LiAl has the $B32$ (NaTl) structure [see Fig. 1(b)] with an underlying bcc lattice. Beyond $x = \frac{1}{2}$ other first-order transitions take place, to the so-called "interloper" phases Al_2Li_3 (space group $R3m$) and Al_4Li_9 (space group $C2/m$), which have neither the fcc nor bcc underlying lattice type. Finally at $x = 1$, bcc Li is observed. Sluiter *et al.*[3] have calculated cohesive energies

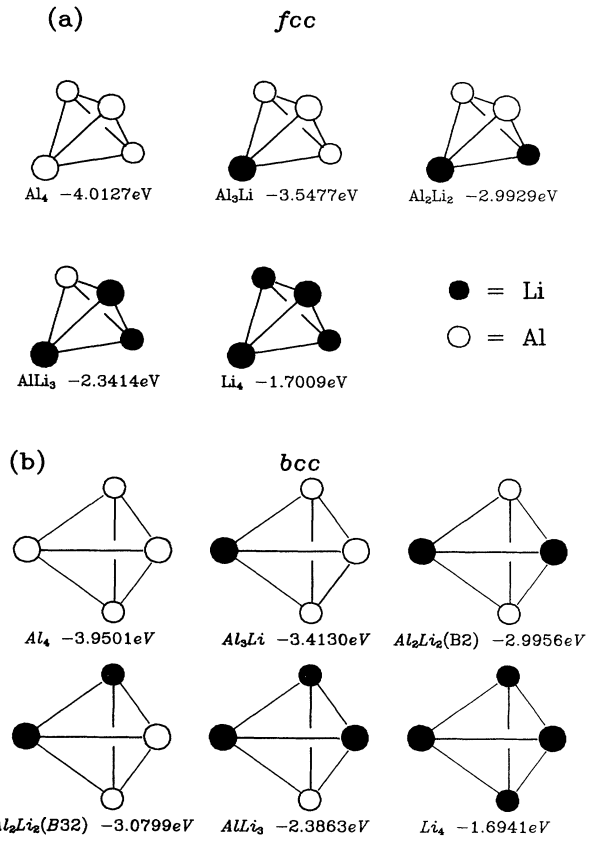

FIG. 1. (a) Various atomic arrangements for one fcc unit cell of Li_xAl_{1-x} for $x=0,1/4,1/2,3/4,1$. (b) As in (a) for two bcc unit cells. The *ab initio* cohesive energies (per atom) as calculated by Sluiter *et al.* (Ref. 3) are listed below each cluster.

for a number of four-site Li_xAl_{1-x} cluster configurations, for both fcc and bcc lattice types, using the full-potential linearized augmented-plane-wave (FLAPW) method.[13]

II. INVERSION METHOD OF CONNOLLY AND WILLIAMS

Here we describe how effective atom-atom interactions are obtained from total energies of extended systems with various atom configurations. One unit cell of the fcc lattice is represented by a tetrahedral cluster for which there are five possible configurations, shown in Fig. 1(a), along with the calculated cohesive energies (in eV per atom) for the extended system. Superlattice structures, which cannot be described within this " tetrahedron approximation," such as the interloper phases mentioned above, will not be considered. Following the inversion method of Connolly and Williams,[4] we will express these energies in terms of a lattice-gas model with suitable interaction parameters. In a lattice-gas model each site i is occupied by either Al ($\sigma_i=0$) or Li ($\sigma_i=1$). Then a general expression for the cohesive energy (within the tetrahedron approximation) for one unit cell of the fcc lattice now follows:

$$\begin{aligned}E_{\rm coh}=&4J_0+J_1(\sigma_1+\sigma_2+\sigma_3+\sigma_4)\\&+4J_2(\sigma_1\sigma_2+\sigma_2\sigma_3+\sigma_3\sigma_4+\sigma_4\sigma_1+\sigma_1\sigma_3+\sigma_2\sigma_4)\\&+8J_3(\sigma_1\sigma_2\sigma_3+\sigma_2\sigma_3\sigma_4+\sigma_3\sigma_4\sigma_1+\sigma_4\sigma_1\sigma_2)\\&+8J_4\sigma_1\sigma_2\sigma_3\sigma_4\ .\end{aligned}\tag{2}$$

The prefactors for the two-, three-, and four-body terms result from periodic boundary conditions around the cluster. Using the rule $\sigma_i=0$ if site i is occupied by Al and $\sigma_i=1$ for Li, the cohesive energies, listed in Fig. 1(a), in terms of the five interaction parameters are

$$\begin{aligned}&Al_4 && E_{\rm coh}=4(-4.0127\ \text{eV})=4J_0\ ,\\&Al_3Li && E_{\rm coh}=4(-3.5477\ \text{eV})=4J_0+J_1\ ,\\&Al_2Li_2 && E_{\rm coh}=4(-2.9929\ \text{eV})=4J_0+2J_1+4J_2\ ,\\&AlLi_3 && E_{\rm coh}=4(-2.3414\ \text{eV})\\&&&\quad=4J_0+3J_1+12J_2+8J_3\ ,\\&Li_4 && E_{\rm coh}=4(-1.7009\ \text{eV})\\&&&\quad=4J_0+3J_1+24J_2+32J_3+8J_4\ .\end{aligned}\tag{3}$$

Solving for the J's gives $J_0=-4.012\,70$ eV, $J_1=1.860\,00$ eV, $J_2=0.089\,80$ eV, $J_3=0.003\,45$ eV, and $J_4=-0.057\,30$ eV.

A similar procedure must be carried out for the bcc lattice for which a tetrahedral cluster is actually made up of two unit cells and is distorted. The six distinct configurations are shown in Fig. 1(b). Here, first- ($J_{2,1}$) and second- ($J_{2,2}$) neighbor two-body interactions are included corresponding to bond distances $\sqrt{3}a/2$ and a respectively, where a is the unit-cell edge. The resulting energy expression and interaction parameters for the bcc case are

$$\begin{aligned}E_{\rm coh}=&4J_0+J_1(\sigma_1+\sigma_2+\sigma_3+\sigma_4)\\&+4J_{2,1}(\sigma_1\sigma_2+\sigma_2\sigma_3+\sigma_3\sigma_4+\sigma_4\sigma_1)\\&+6J_{2,2}(\sigma_1\sigma_3+\sigma_2\sigma_4)\\&+12J_3(\sigma_1\sigma_2\sigma_3+\sigma_2\sigma_3\sigma_4+\sigma_3\sigma_4\sigma_1+\sigma_4\sigma_1\sigma_2)\\&+24J_4\sigma_1\sigma_2\sigma_3\sigma_4\end{aligned}\tag{4}$$

with $J_0=-3.950\,10$ eV, $J_1=2.148\,40$ eV, $J_{2,1}=-0.204\,00$ eV, $J_{2,2}=-0.079\,80$ eV, $J_3=0.160\,07$ eV, and $J_4=-0.126\,30$ eV.

Configurational entropy must now be considered along with the energy expressions (2) and (4) to predict finite temperature physical properties.

III. SOLUTION OF THE STATISTICAL MECHANICS

A. Calculating voltage

The next step in determining the voltage curve of an electrochemical cell is to solve the statistical mechanics of the lattice gas model. Below we will describe the two methods used in this work, the mean-field approximation and the Monte Carlo method. The lattice gas model is

most conveniently described in terms of the composition x in Li_xAl_{1-x}. On the other hand, experimental measurements are carried out as a function of y in Li_yAl, where $y=x/(1-x)$. In this section we describe how the Li chemical potentials (and hence voltages) of the two systems are related.

In an experimental Li/Li_yAl cell the amount of aluminum is fixed, and manipulations are required to obtain the measured voltage $V(y)$ in (1) as a function of μ (for Li in Li_xAl_{1-x}). First we must introduce the Helmholtz potential[14]

$$F(x,T)=\langle E_{\rm coh}\rangle - TS=\Omega(\mu,T)+N\mu x \ , \tag{5}$$

of Li_xAl_{1-x}, where N is the number of available sites to be filled by Li or Al. Similarly

$$F'(y,T)=\Omega'(\mu',T)+N'\mu'y' \ , \tag{6}$$

for Li_yAl, where N' is the number of Al atoms. Since $\mu'(y)=(1/N')(\partial F'/\partial y)$, we have

$$eV(y)=\mu_{\rm Li}-(1/N')(\partial F'/\partial y) \ , \tag{7}$$

where $\mu_{\rm Li}$ is the chemical potential of lithium metal. The free energies of

$$\frac{1}{1-x}(Li_xAl_{1-x}) \text{ and } Li_{x/(1-x)}Al \tag{8}$$

must be equal therefore, to

$$\frac{1}{1-x}F(x,T)=F'\left[\frac{x}{1-x},T\right]=F'(y,T) \ . \tag{9}$$

Then

$$\frac{\partial F'}{\partial y}=\frac{dx}{dy}\frac{d}{dx}\left[\frac{1}{1-x}F(x,T)\right]=(1-x)\frac{\partial F}{\partial x}+F(x,T) \ . \tag{10}$$

The Helmholtz free energy of Li_xAl_{1-x} is $F(x,T)=\Omega(\mu,T)+N\mu x$; therefore, using (7),

$$eV(y,T)=\mu_{\rm Li}-\Omega(\mu,T)/N-\mu \ . \tag{11}$$

We use Eq. (11) and $y=x/(1-x)$ to calculate voltage curves, which can be compared with experiment.

B. Mean-field approximation

Mean-field theory approximates many-body correlations as a product of one-body expectation values, $\langle x_ix_j\rangle\approx\langle x_i\rangle\langle x_j\rangle$. One can show that the mean-field entropy for a lattice gas is[15]

$$S=-k_B\sum_i[x_i\ln x_i+(1-x_i)\ln(1-x_i)] \ , \tag{12}$$

where k_B is Boltzmann's constant ($k_B=8.6173\times10^{-4}$ eV/K) and the summation is over the four sites in the tetrahedral cluster. The grand potential Ω is

$$\Omega(\mu,T)=\langle E_{\rm coh}\rangle - N\mu x - TS \ , \tag{13}$$

where N is the number of lattice sites, μ is the chemical potential of Li in Li_xAl_{1-x} and

$$x=\frac{1}{N}\sum_i x_i \tag{14}$$

is the average occupation by Li of all sites. We wish to minimize the grand potential Ω with respect to the average occupations x_i:

$$\frac{\partial\Omega}{\partial x_i}=\varepsilon_i-\mu+k_BT\ln\left[\frac{x_i}{1-x_i}\right]=0 \ , \quad i=1,\ldots,4 \tag{15}$$

or

$$x_i=\{1+\exp[(\varepsilon_i-\mu)/(k_BT)]\}^{-1} \tag{16}$$

The derivatives ε_i depend on lattice type and i, that is for fcc

$$\begin{aligned}\varepsilon_1=&\frac{\partial\langle E_{\rm coh}\rangle}{x_1}\\ &+J_1+4J_2(x_2+x_3+x_4)+8J_3(x_2x_3+x_3x_4+x_4x_2)\\ &+8J_4x_2x_3x_4 \ ,\end{aligned} \tag{17}$$

and for bcc

$$\begin{aligned}\varepsilon_1=&\frac{\partial\langle E_{\rm coh}\rangle}{x_1}\\ =&J_1+4J_{2,1}(x_2+x_4)\\ &+6J_{2,2}x_3+12J_3(x_2x_3+x_3x_4+x_4x_2)\\ &+24J_4x_2x_3x_4 \ .\end{aligned} \tag{18}$$

Other derivatives are obtained by cyclic permutation of the indices.

The system of equations (16) is nonlinear and must be solved numerically. For simplicity we chose a simple iterative scheme, which stops when the system of equations (16) is self-consistent to within a prescribed numerical tolerance (in our case $|\Delta x|=|x_{\rm old}-x_{\rm new}|<10^{-13}$). We start with a small μ and an initial guess $x_i=0$ and iterate Eq. (16) until convergence is achieved. μ is then increased by some suitable increment $\Delta\mu$, and the iteration is repeated using the preceding solution as an initial guess. This ramping up of μ and using the previous solution as an initial guess can lead to complications if the grand potential Ω develops multiple minima, since the iteration scheme will only find the nearest minimum to the initial guess. At small μ we know that all $x_i\approx0$ is the only minimum of Ω. In order to find the global minimum at each μ, we carry out the whole calculation twice by first ramping up in μ as described above and then ramping down starting with $x_i\approx1$ as an initial guess at large μ. The results for both calculations for each μ are compared, and the one with the lowest grand potential Ω is selected as the equilibrium solution.

As an example of the results of such a calculation we show the average sublattice occupations x_i and the total occupation x as functions of the chemical potential μ at $T=300$ K for the fcc lattice in Fig. 2. The numbers next to each line indicate the number of sublattices with that composition. As μ increases, more and more sublattices become predominantly occupied by lithium.

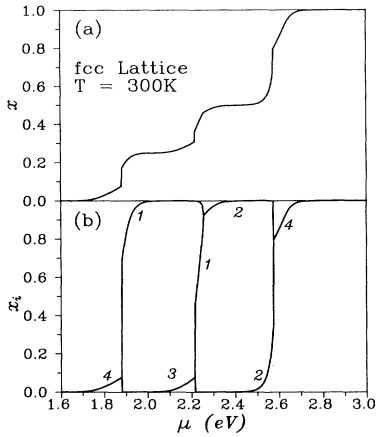

FIG. 2. (a) The overall average occupation of Li [Eq. (14)] in Li_xAl_{1-x} as a function of the chemical potential μ. (b) As in (a) except for the four individual sublattices.

In Fig. 3 we show the *ab initio* voltage vs composition ($y=x/[1-x]$) curves for the fcc and bcc lattices obtained by iteratively solving (16) for a suitable range of chemical potentials μ at $T=300$ K. The fcc curve is very steep at $y=\frac{1}{3}$ and $y=1$, which corresponds to ordered phases[16] at $x=\frac{1}{4}$ and $x=\frac{1}{2}$, respectively. The bcc curve exhibits a wide plateau from $0\leq y\leq 1$, which results from the phase coexistence of bcc Al and $B32$ LiAl.

The final step is to combine the fcc and bcc results by selecting the lattice with the lowest Ω at constant μ. The grand potentials for both lattices are shown in Fig. 4, where some hysteresis for the bcc lattice is evident. Below $\mu\approx 1.9$ eV the fcc structure is preferred, and for $\mu>1.9$ eV the bcc structure is preferred. The switch from fcc to bcc at $\mu=1.9$ eV involves a large change in composition, $\Delta y\approx 1$. The final mean-field-theory voltage curve is shown in Fig. 5(a) for $T=300$ K.

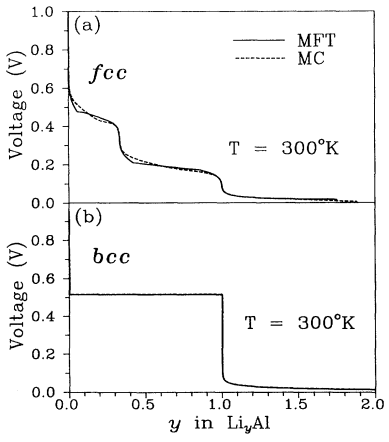

FIG. 3. Equilibrium voltage curves for fcc (a) and bcc (b) Li_yAl as calculated using mean-field theory and Monte Carlo at 300 K.

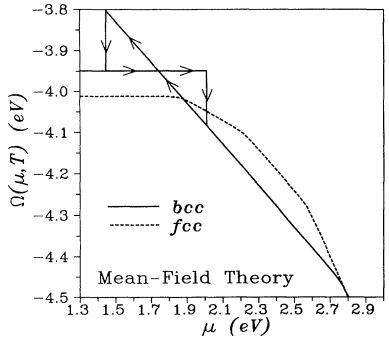

FIG. 4. The grand potential $\Omega(\mu,T)$ form both fcc and bcc lattice types, calculated using mean field theory.

C. Monte Carlo method

The mean-field approximation often distorts the results near critical points and more importantly, for our purpose, it shifts critical points from their true values. Therefore, we have recalculated all quantities using the Monte Carlo technique.[17] Monte Carlo makes no approximations for the many-body correlations but does suffer from finite-size effects and statistical noise. These problems are most severe when calculating fluctuation quantities such as heat capacity and susceptibility. For our purposes no fluctuation quantities are required, just the free energy and x. Calculation of the free energy by Monte Carlo is complicated because the free energy cannot be expressed as the expectation value of an observable.[17] We use Ferrenberg's and Swendsen's multiple histogram method,[18] which allows one to obtain accurate estimates of the free energy and all other quantities as continuous functions of μ. Histograms where calculated for 171 values of μ in the range $1.5\leq\mu\leq 3.2$, which encompasses the whole range of $0\leq x\leq 1$ (or $0\leq y\leq\infty$) for both lattices. The simulation lengths were 10 000 Monte Carlo steps per site for each μ. As in the mean-field calculations, the simulations were done twice by ramping μ both up and down in order to find the equilibrium behavior.

The calculations were carried out for a $4\times4\times4$ unit-

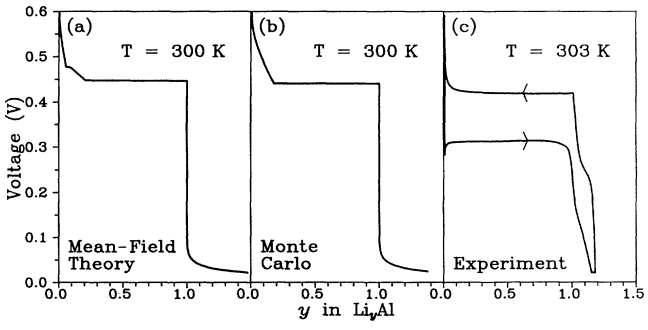

FIG. 5. The final mean field (a), Monte Carlo (b), and measured (c) voltage curves for Li_yAl at room temperature. Measured charge and discharge cycles are labeled by the arrows.

cell lattice, which corresponds to 256 and 128 sites for the fcc and bcc lattices, respectively. The bcc lattice is dominated by a very strong first-order transition for which there can be no finite-size effects. On the other hand, the fcc lattice exhibits three apparently continuous transitions, which will suffer from finite-size effects in our simulations. The discrepancy in calculated voltages between $4\times4\times4$ and $8\times8\times8$ fcc lattices was found to be less 0.005 V. Also none of these continuous transitions are relevant to our final result, as they are preempted by a transition to the bcc underlying lattice.

The fcc and bcc Monte Carlo voltage curves are shown as dashed lines in Fig. 3. For the bcc lattice, mean-field theory and Monte Carlo give essentially identical results. The final Monte Carlo equilibrium voltage curve is shown in Fig. 5(b).

IV. COMPARISON WITH EXPERIMENT

The final test is to compare these results with experiment. Accurate voltage measurements were carried out on a Li/Li_yAl coin cell[19] using 1 M $LiN(CF_3SO_2)_2$ in a 50:50 volume mixture of propylene carbonate and ethylene carbonate. The cell was charged and discharged using a constant current cycler and thermostated at 30 °C. Data were logged whenever the cell voltage changed by more than 0.002 V. The charging and discharging currents corresponded to a change of $\Delta y=1$ in Li_yAl in 200 h. The aluminum anode surface was scraped in an argon atmosphere in an attempt to remove the Al_2O_3 passivation layer. A typical charge-discharge cycle is shown in Fig. 5(c). Values of y were obtained using the mass of Al initially incorporated in the cell, the constant current and the duration of current flow.

The comparison with the measured voltage curve is complicated by the fact that the experimental system exhibits strong hysteresis in the fcc Al-$B32$ LiAl coexistence region. The agreement between the theory and measured recharge is remarkable, the plateau voltage being accurate to within ≈10 mV. For $0\le y\le0.2$ the calculations predict an fcc structure, and for $0.2\le y\le1.0$ there is a phase coexistence between fcc and bcc structures. The narrow plateau at $y=1.1$ in the measured data is due to the Al_2Li_3 interloper phase, which was not included in the calculations. However, if total or cohesive energies were available for various atom configurations of the rhombohedral Al_2Li_3 structure, then inclusion of this phase in the calculation would be straightforward. The calculation also predicts that the charge curve is near equilibrium, suggesting that strain or interface energies (which to our knowledge have not been calculated *ab initio*) are suppressing nucleation of the $B32$ LiAl phase from fcc Li_xAl on discharge.

This could be tested experimentally using a battery calorimeter. If a cell is charged or discharged with a constant current in a sensitive, isothermal, calorimeter, the heat flow out of the cell due to hysteresis is equal to the difference between the cell voltage and the equilibrium voltage multiplied by current.[20] There is unfortunately, a second term in the calorimeter heat flow, which is proportional to the current.[20] This term depends on the change of the partial molar entropy with y in Li_yAl. If the entropy of $B32$ LiAl and fcc Al are accurately known, one can separate the hysteresis and entropy contributions thus obtaining the equilibrium voltage. If the entropy term is small, and if there is no hysteresis present during the charging of the Li/Li_yAl cell, the charge should show much less heat output than the discharge.

V. CONCLUSIONS

We have shown that accurate *ab initio* calculations of voltage curves for electrochemical cells are possible. The rate limiting step is the calculation of total energies from which the effective atom-atom interactions are derived. Such calculations on technologically important intercalation compounds, such as graphite,[8] boronated graphite,[8] $LiNiO_2$,[9] $LiCoO_2$,[10] and $LiMn_2O_4$,[11] would provide deeper insight into the physical properties of the host material that determine electrochemical behavior. As more experience and confidence is gained in these calculations, *ab initio* methods may also provide a useful presynthesis screening mechanism for candidate electrode materials to be used in advanced battery applications.

ACKNOWLEDGMENTS

This work has benefited from useful discussions with Professor D. deFontaine, W. R. McKinnon, and R. Magri. Financial assistance for J.R.D. and J.N.R. was provided by the Natural Sciences and Engineering Research Council of Canada.

[1]W. Y. Ching, J. Am. Ceram. Soc. **73**, 3135 (1990).

[2]C. Sigli, M. Kosugi, and J. M. Sanchez, Phys. Rev. Lett. **57**, 253 (1986); M. Sluiter, P. Turchi, Fu Zezhong, and D. de Fontaine, Phys. Rev. Lett. **60**, 716 (1988); P. Turchi, M. Sluiter, and D. de Fontaine, Phys. Rev. B **36**, 3161 (1987).

[3]M. Sluiter, D. de Fontaine, X. Q. Guo, R. Podloucky, and A. J. Freeman, Phys. Rev. B **42**, 10460 (1990).

[4]J. W. Connolly and A. R. Williams, Phys. Rev. B **27**, 5169 (1983).

[5]S. T. Coleman, W. R. McKinnon, and J. R. Dahn, Phys. Rev. B **29**, 4147 (1984); J. R. Dahn and W. R. McKinnon, J. Phys. C **17**, 4231 (1984).

[6]W. R. McKinnon and R. R. Haering, in *Modern Aspects of Electrochemistry,* edited by R. E. White, J. O'M. Backris, and B. E. Conway (Plenum, New York, 1983), Vol. 15, p. 235.

[7]C. J. Wen, B. A. Boukamp, R. A. Huggins, and W. Weppner, J. Electrochem. Soc. **135**, 2258 (1979).

[8]J. R. Dahn, Phys. Rev. B **44**, 9170 (1991).

[9]J. R. Dahn, U. von Sacken, M. W Juzkow, and H. Al-Janaby, J. Electrochem. Soc. **138**, 2207 (1991).

[10]K. Mizushima, P. C. Jones, P. J. Wiseman, and J. B. Goodenough, Mater. Res. Bull. **15**, 783 (1980).

[11]D. Guyomard and J. M. Tarascon, J. Electrochem. Soc. **139**, 937 (1992).

[12]A. J. McAlister, Bull. Alloy Phase Diagrams **3**, 177 (1982).
[13]H. J. F. Jansen and A. J. Freeman, Phys. Rev. B **30**, 561 (1984).
[14]Although the Gibbs function $G=F+PV$ is generally used by electrochemists, we are not including any volume effects in our calculation, since the pressure is only 1 atm, and we are therefore using the Helmholtz potential F.
[15]W. L. Bragg and E. J. Williams, Proc. R. Soc. London, Ser. A **145**, 699 (1934); J. N. Reimers and J. R. Dahn, J. Phys. Condens. Matter **4**, 8105 (1992).
[16]A. J. Berlinsky, W. G. Unruh, and W. R. McKinnon, Solid State Commun. **31**, 175 (1979).
[17]*Applications of the Monte Carlo Method in Statistical Physics,* Topics in Current Physics Vol. 7, edited by K. Binder (Springer, New York, 1987), see p. 7 for a discussion of the problems associated with calculating free energies.
[18]A. M. Ferrenberg and R. H. Swendsen, Phys. Rev. Lett. **61**, 2635 (1988); **63**, 1195 (1988); Comput. Phys. **3**, 101 (1989).
[19]J. R. Dahn, R. Fong, and M. J. Spoon, Phys. Rev. B **42**, 6424 (1990).
[20]W. R. McKinnon, J. R. Dahn, J. J. Murray, R. R. Haering, R. S. McMillan, and A. H. Rivers-Bowerman, J. Phys. C **19**, 5135 (1986).